Supporting Information

Light-induced puromycin release from a coumarin-caged compound on the ultrafast timescale

Lisa-Marie Herzig,[(1)] *Isam Elamri,*[(2)] *Harald Schwalbe,*[(2)] *Josef Wachtveitl*[(1)]

[(1)] Institute of Physical and Theoretical Chemistry, Center for Biomolecular Magnetic Resonance (BMRZ), Goethe University Frankfurt, Max-von-Laue Str. 7, 60438 Frankfurt/Main, Germany
[(2)] Institute of Organic Chemistry and Chemical Biology, Goethe University Frankfurt, Max-von-Laue Str. 7, 60438 Frankfurt/Main, Germany

Contents

Additional experiments

Monitoring uncaging with rp-HPLC and analysis of uncaging products

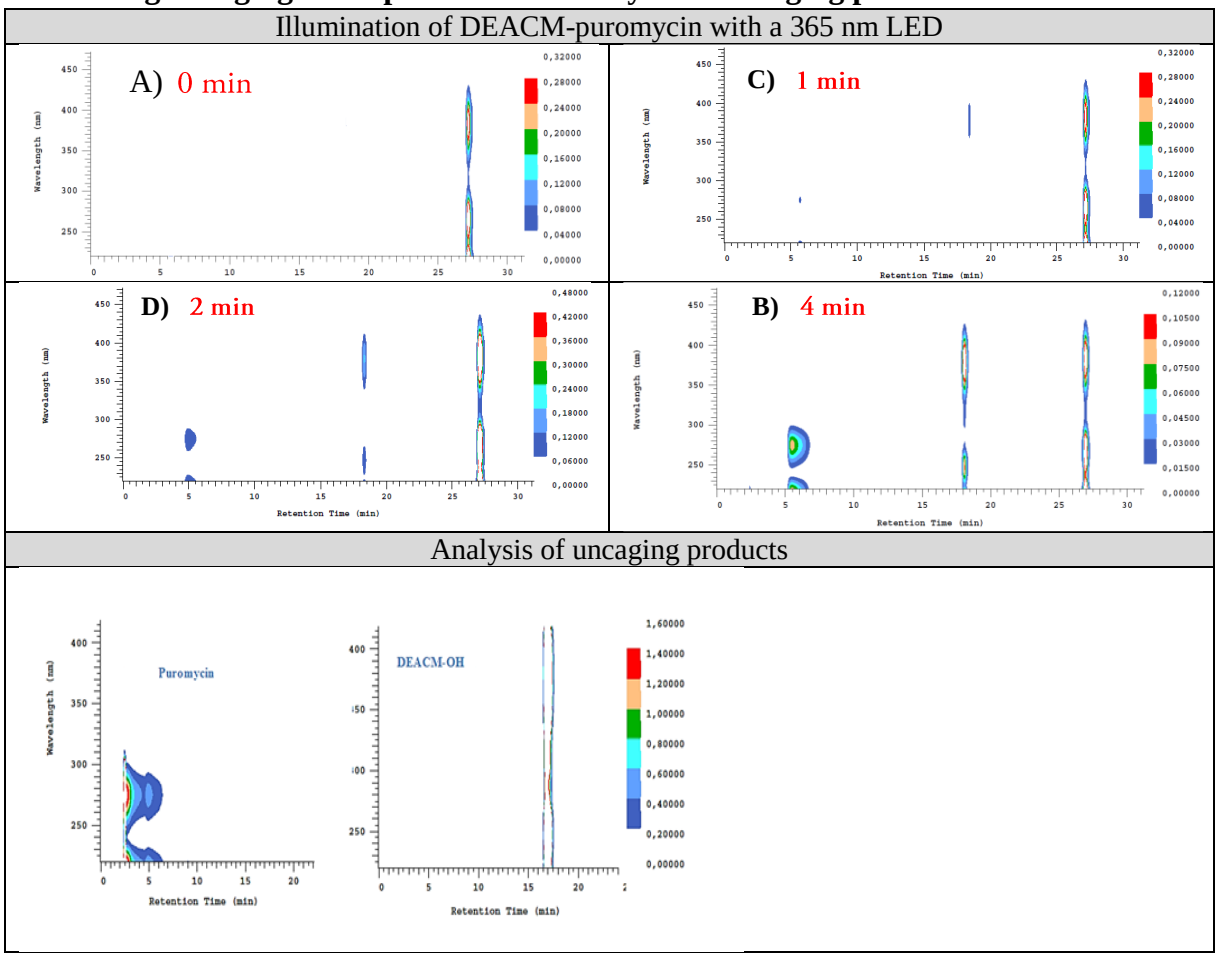

Figure S1: Tracing the uncaging of DEACM-puromycin with rp-HPLC, A) 0 min, B) 1 min, C) 2 min D) 4 min of illumination with a 365 nm LED (500 mA, 250 mW). Analysis of the uncaging products.

Determination of extinction coefficients

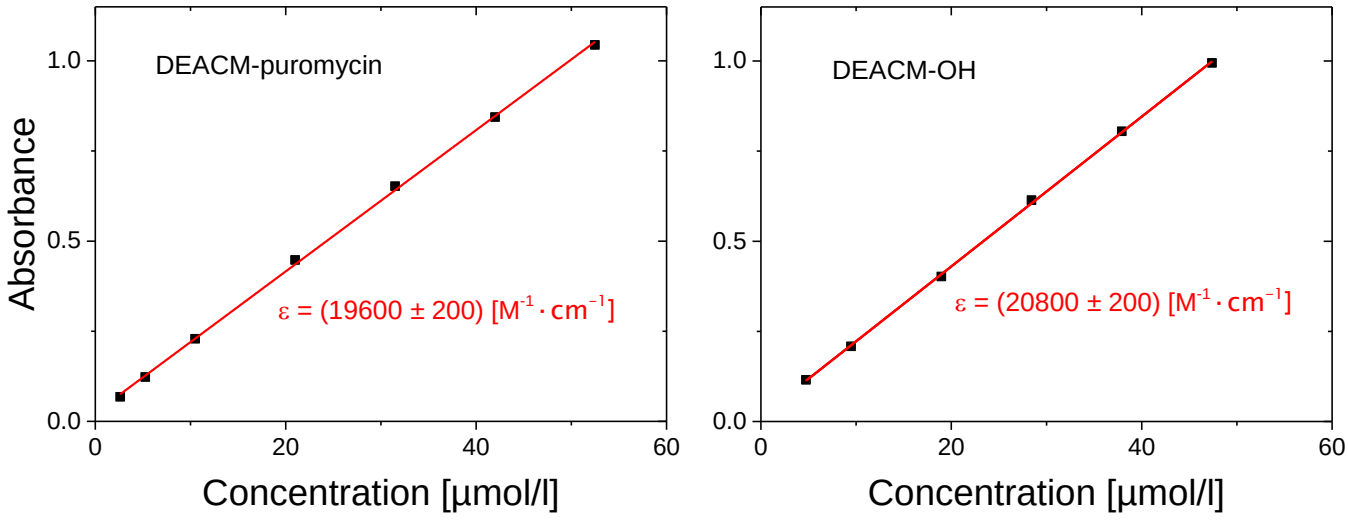

Figure S2. Determination of the molar extinction coefficients of DEACM-puromycin and DEACM-OH in pure DMSO at the respective absorption maximum.

Determination of fluorescence quantum yield

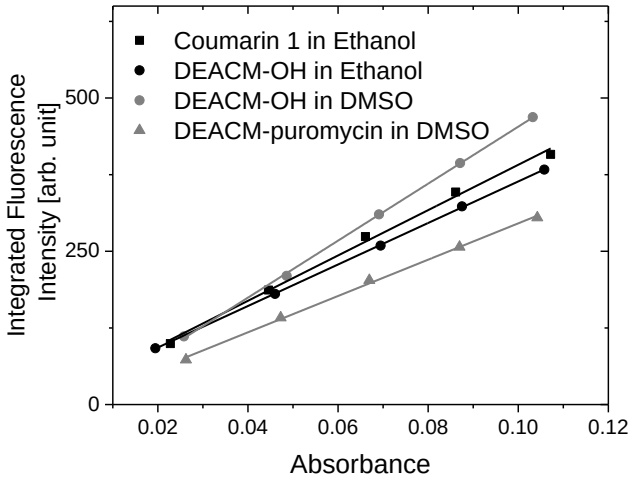

Figure S3. Integrated fluorescence intensities upon 388 nm excitation of Coumarin1 and DEACM-OH in Ethanol, as well as DEACM-OH and DEACM-puromycin in DMSO.

compound	**solvent**	**refractive index**	**gradient**	**R^2**	**ϕ^{fl}**
Coumarin1	Ethanol	1.3605	3700 ± 140	0.997	0.50
DEACM-OH	Ethanol	1.3605	3390 ± 20	0.999	0.46
DEACM-OH	DMSO	1.4775	4650 ± 50	0.999	0.74
DEACM-puromycin	DMSO	1.4775	2960 ± 70	0.999	0.47

The fluorescence quantum yield of DEACM-OH was determined relative to Coumarin1 as reference compound in Ethanol. The obtained fluorescence quantum yield of DEACM-OH in Ethanol was serving as reference for the quantum yield of DEACM-OH and DEACM-puromycin in DMSO. The fluorescence measurement were conducted using 388 nm excitation light. The fluorescence spectra have been corrected considering reabsorption, absorption at the excitation wavelength and inner filter effects. To ensure linear response on the intensity, the concentration of every sample was approximately 5 µM and was serving as the highest concentration for a serial dilution. Then the fluorescence quantum yield was calculated according to:

$$\phi_x^{fl} = \phi_{ref}^{fl} \cdot \left(\frac{gradient_x}{gradient_{ref}}\right) \cdot \left(\frac{\eta_x^2}{\eta_{ref}^2}\right)$$

where ϕ_{ref}^{fl} is the quantum yield of Coumarin1 in Ethanol (0.50) and η the refractive index.

Fluorescence lifetimes of DEACM-puromycin und DEACM-OH depending on amount of water in the solvent

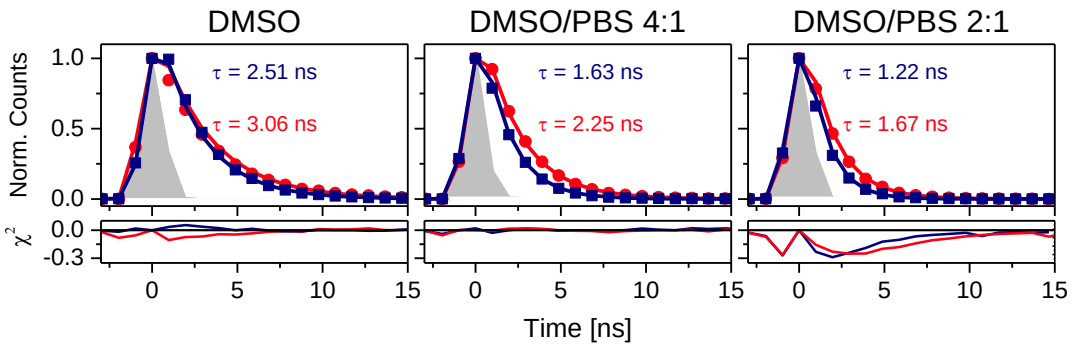

Figure S4: Fluorescence lifetimes of DEACM-puromycin (red) and DEACM-OH (blue) in different solvents, with respective fit quality. The instrumental response function (IRF) is shown in gray.

Table 1: Rate constant for DEACM-puromycin upon excitation

solvent	k_1 [$10^8 \cdot s^{-1}$]
DMSO	0.71
DMSO/PBS[1] 4:1	1.68
DMSO/PBS 2:1	2.25

[1] abbrevation: phosphate buffered saline (PBS), pH =7.4

Spectral changes upon illumination of DEACM-puromycin and DEACM-OH in the IR range

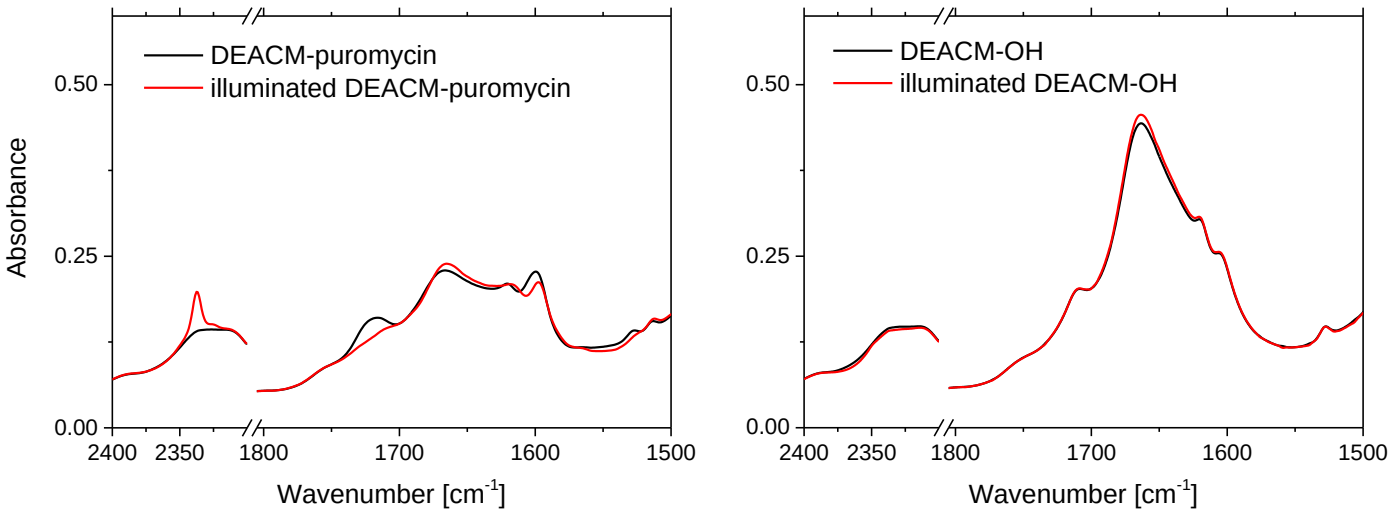

Figure S5: IR spectra before and after excitation of DEACM-puromycin and DEACM-OH in DMSO. The same excitation conditions were applied for both compounds (4 h illumination with 385 nm LED, 5.8 mW, N_2-purging, sample concentrations ~ 8 mM)

Determination of water content in pure DMSO

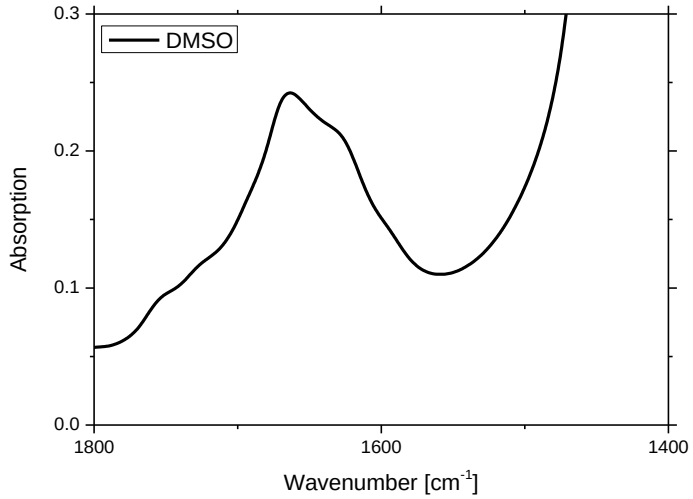

Figure S6. FTIR spectrum of the DMSO used for the experiments. The spectral region shows the range of the H_2O bending vibration of water, which has an absorption coefficient of 2334 cm^{-1} at 1645 cm^{-1} (G. M. Hale and M. R. Querry. Optical Constants of Water in the 200-nm to 200-µm Wavelength Region, Appl. Opt. 12, 555-563 (1973)). With the cuvette thickness of 50 µm this would result in an absorbance of 11.7. The measured absorbance is 0.22. Therefore, the water content is about 2%.

Transient absorption spectrum and respective analysis of DEACM-OH in DMSO

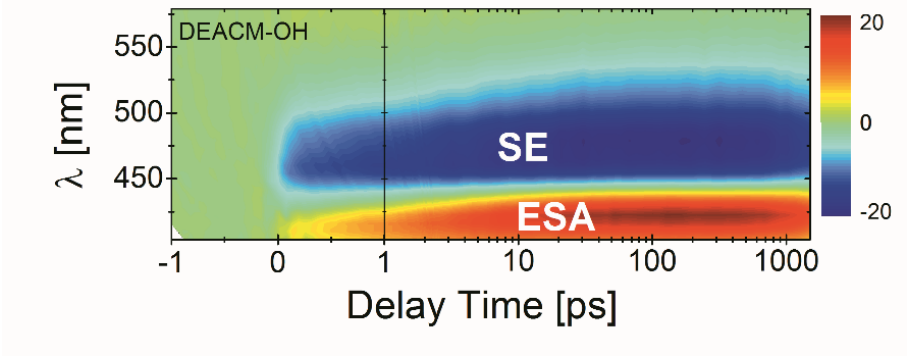

Figure S7. Transient absorption spectrum of DEACM-OH in DMSO upon excitation at 388 nm.

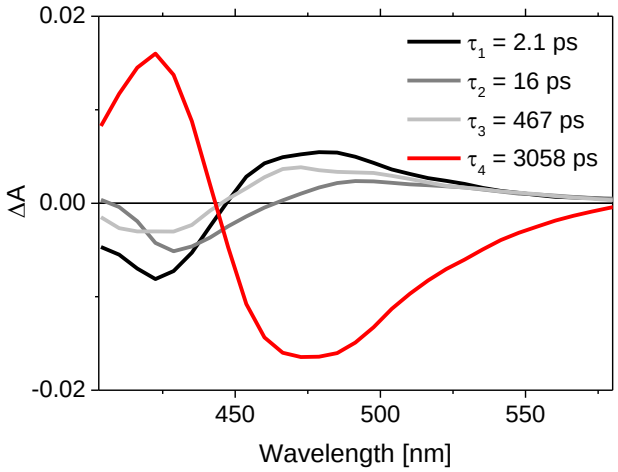

Figure S8. Decay associated spectra with associated exponential time constants resulting from global fit analysis of Figure S6.

Transient absorption spectra and respective analysis of DEACM-puromycin in various solvent mixtures

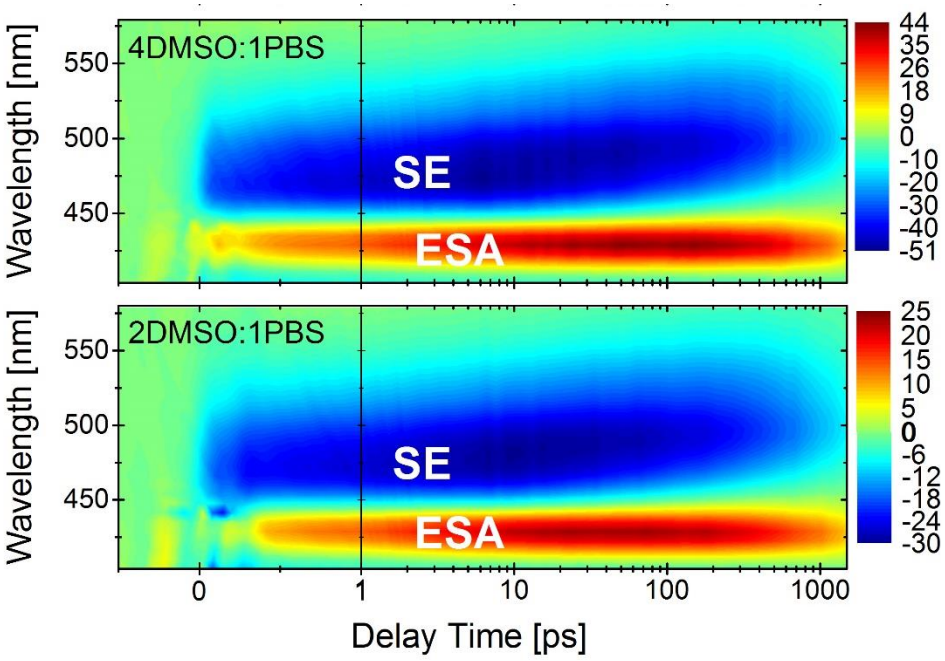

Figure S9: Transient spectra of DEACM-puromycin in different solvent mixtures. Top: DMSO/PBS buffer 4:1. Bottom: DMSO/PBS buffer 2:1.

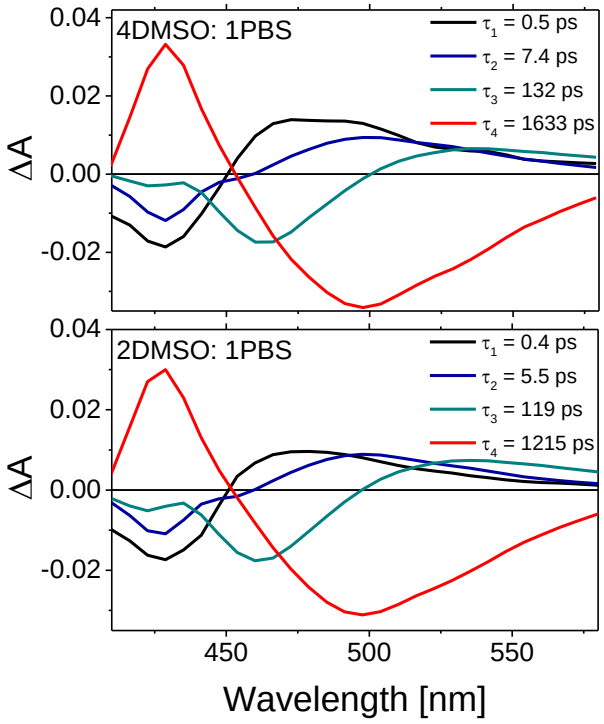

Figure S10: Decay associated spectra of DEACM-puromycin in different solvent mixtures. Top: DMSO/PBS buffer 4:1. Bottom: DMSO/PBS buffer 2:1.

Transient absorption spectrum of DEACM-puromycin in IR range

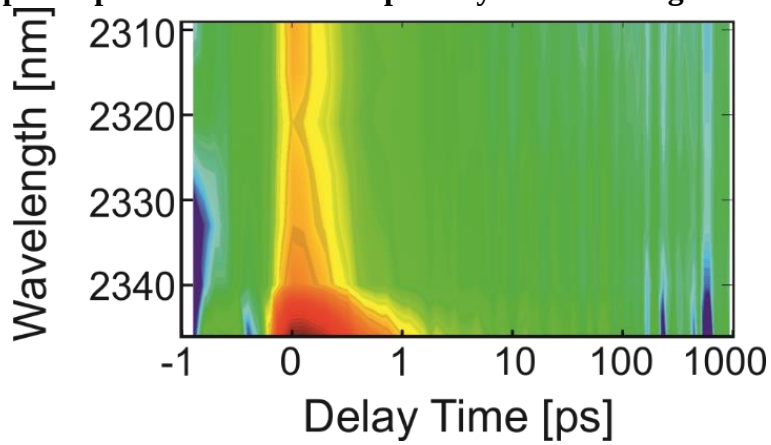

Figure S11. Transient absorption spectra of DEACM-puromycin upon 388 nm excitation and IR detection.

Mulliken population analysis of DEACM-methylacarbamate in S_0 and S_1

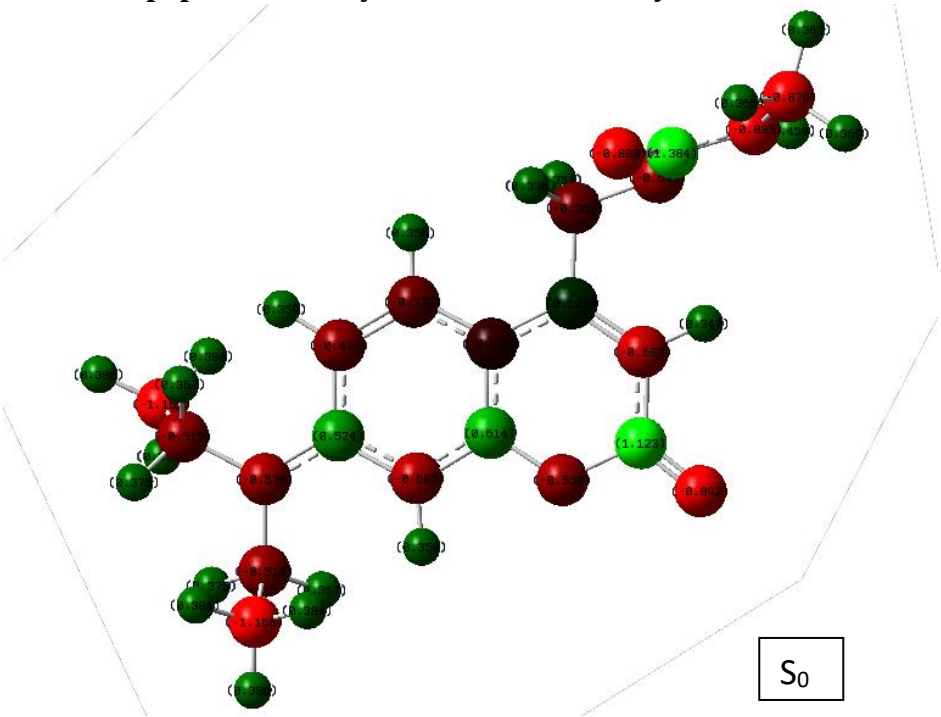

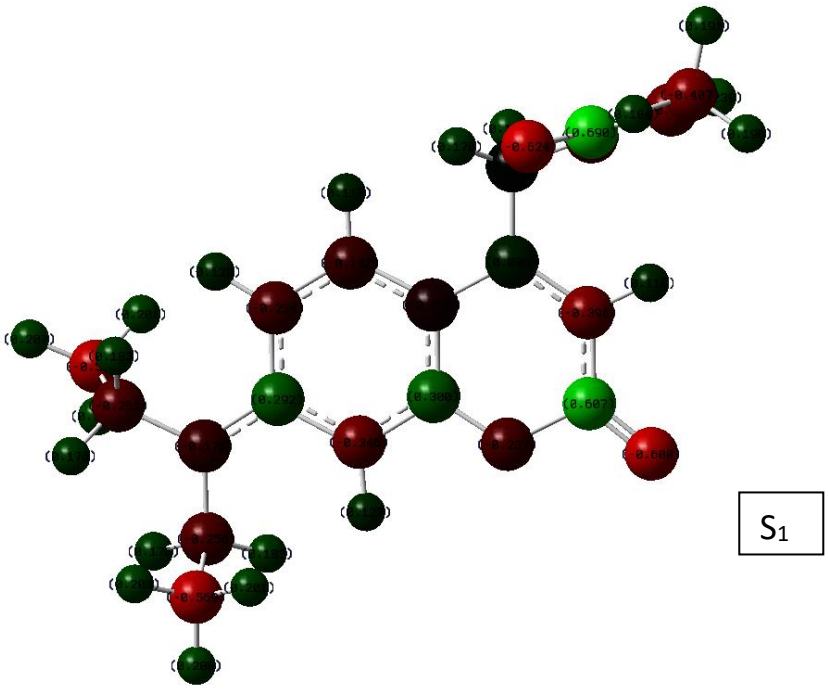

Figure S12: Mulliken population analysis of DEACM-methylcarbamate

NMR and mass spectra

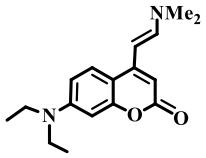

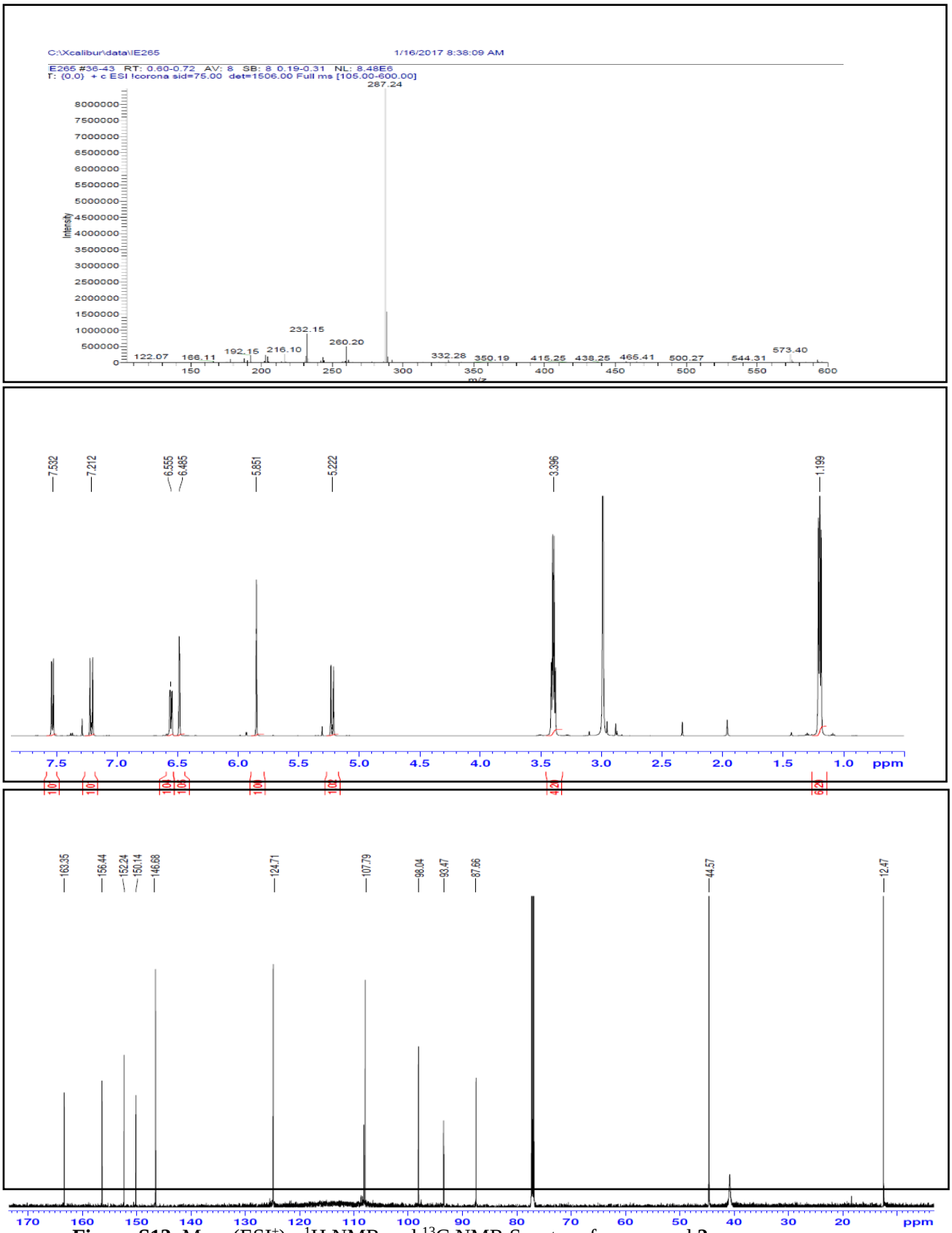

Figure S13. Mass (ESI^+)-, ^1H NMR and ^{13}C NMR Spectra of compound **2**

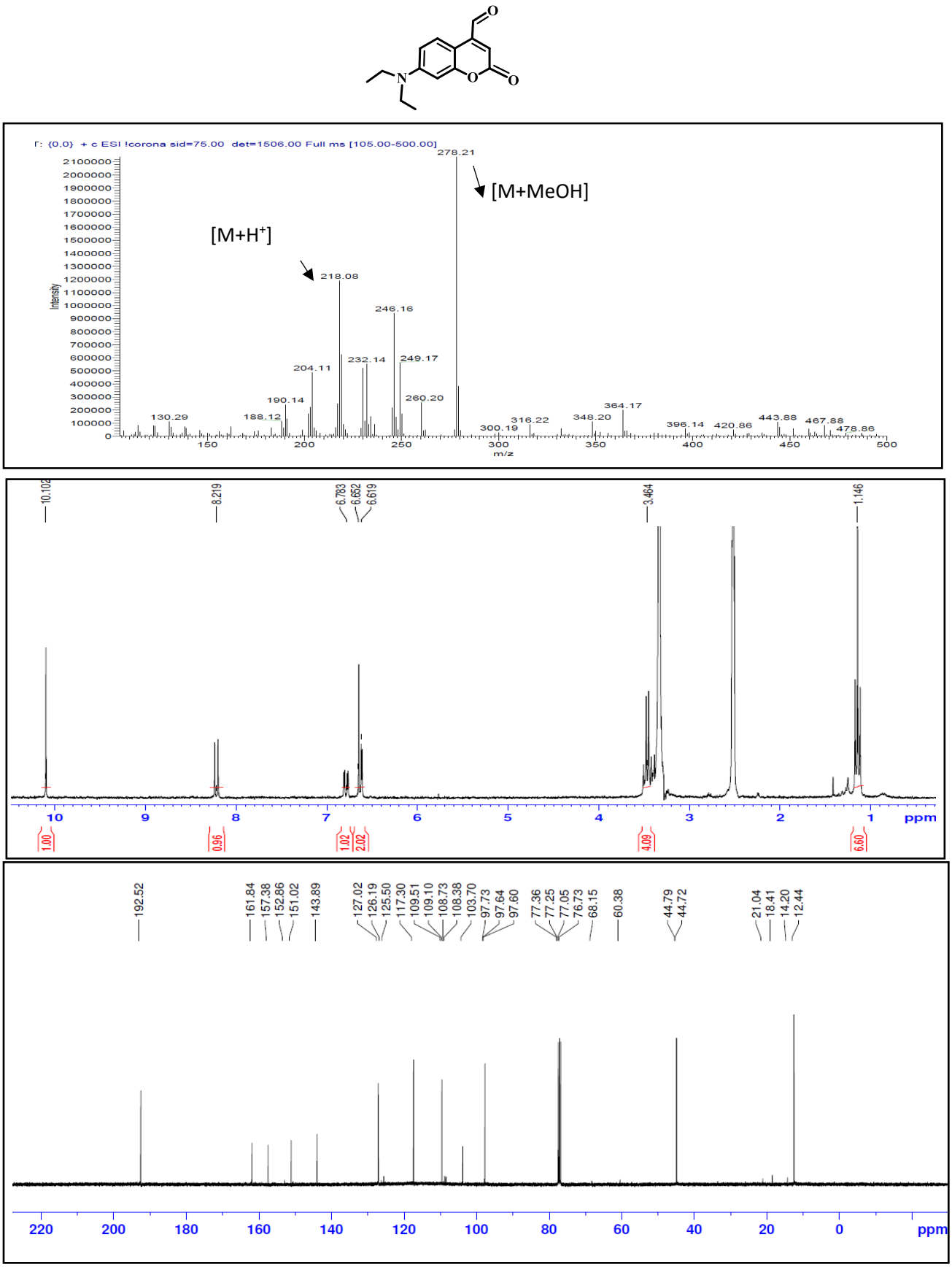

Figure S14. Mass (ESI^+)-, ^1H NMR and ^{13}C NMR spectra of compound **3.**

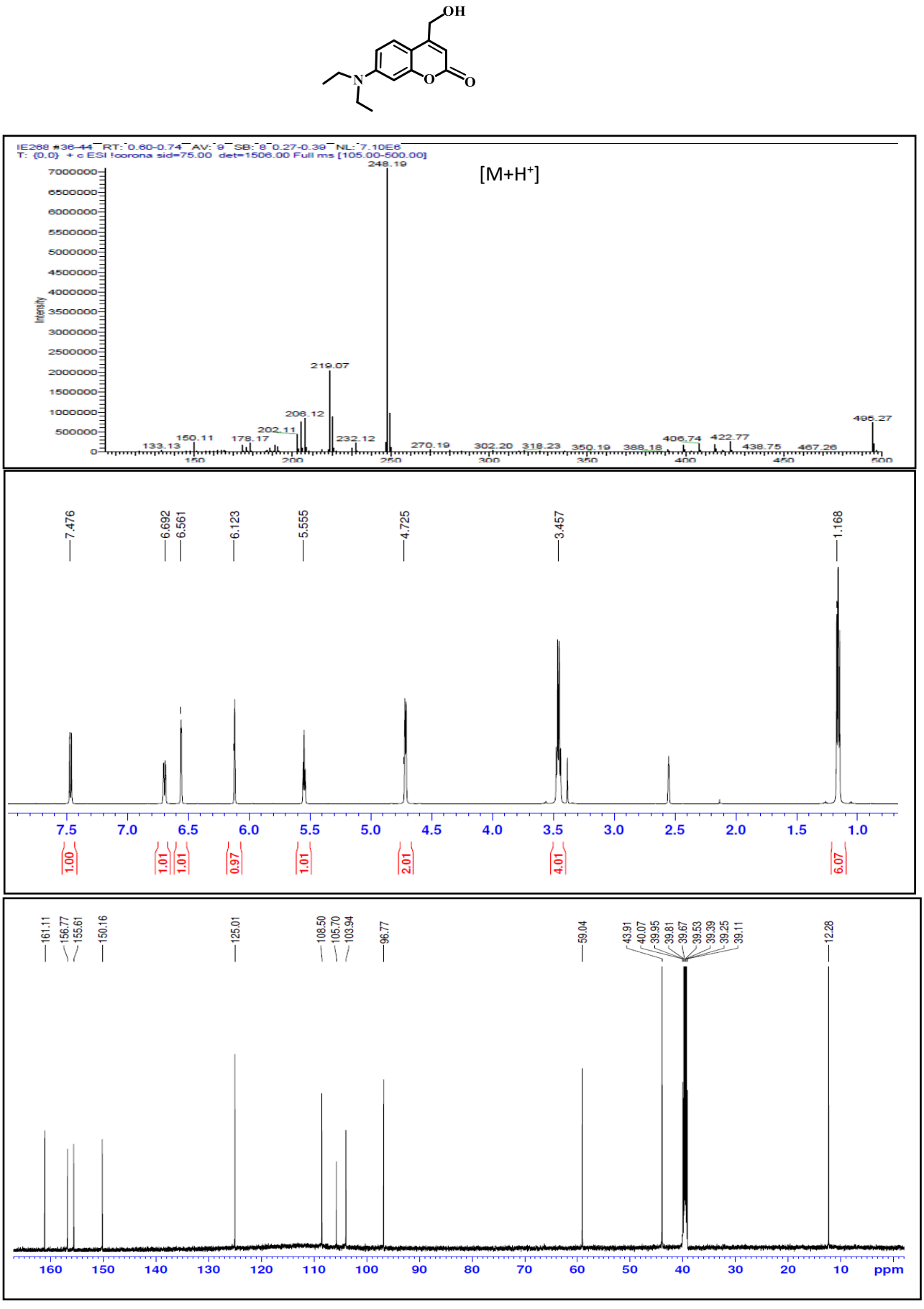

Figure S15. Mass (ESI^+)-, ^1H NMR and ^{13}C NMR Spectra of compound **4.**

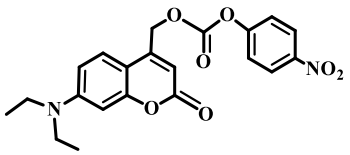

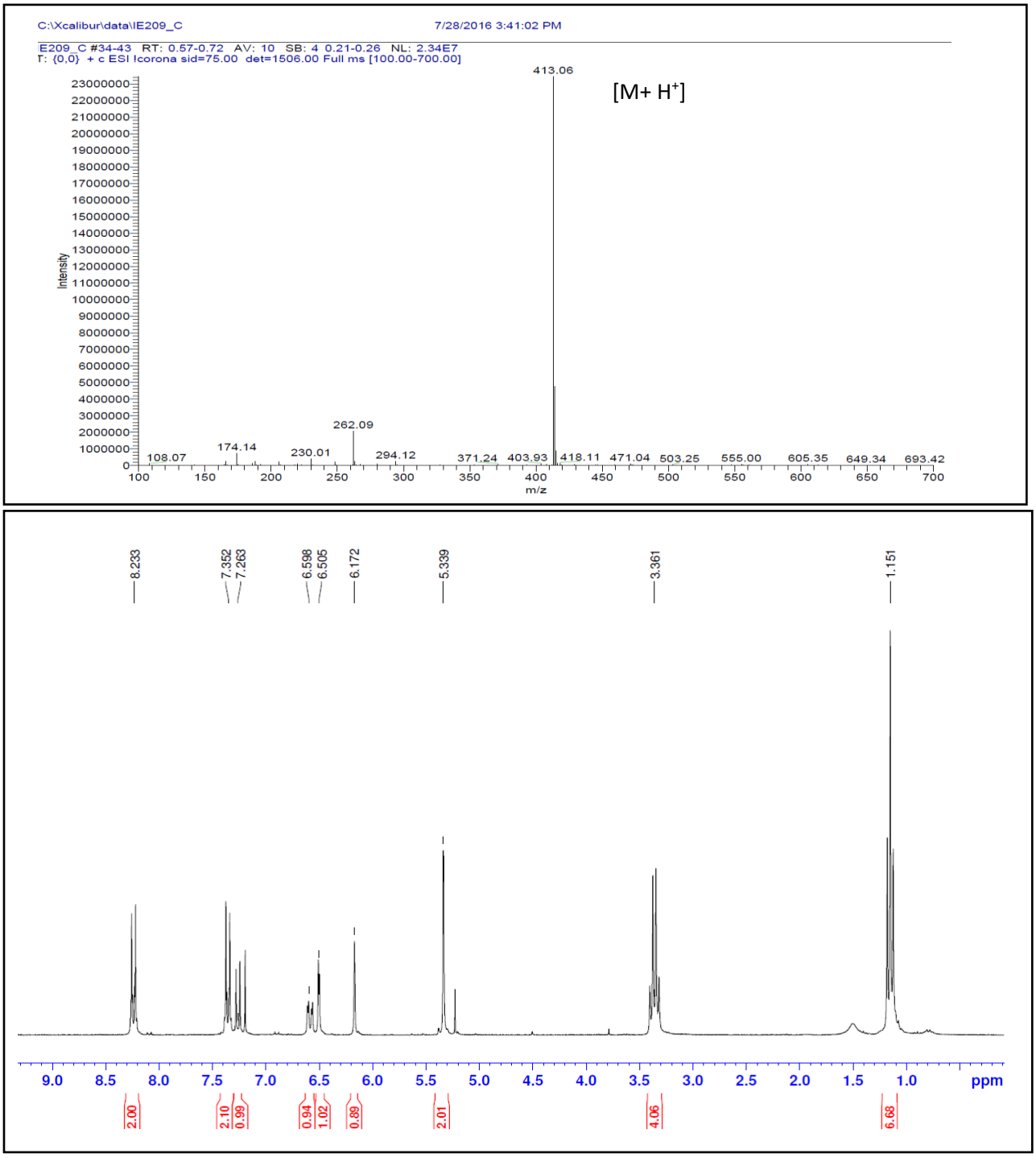

Figure S16. Mass (ESI^+)-, ^1H NMR spectra of compound **5.**

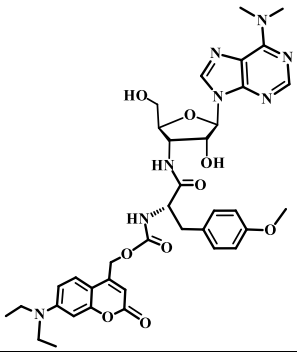

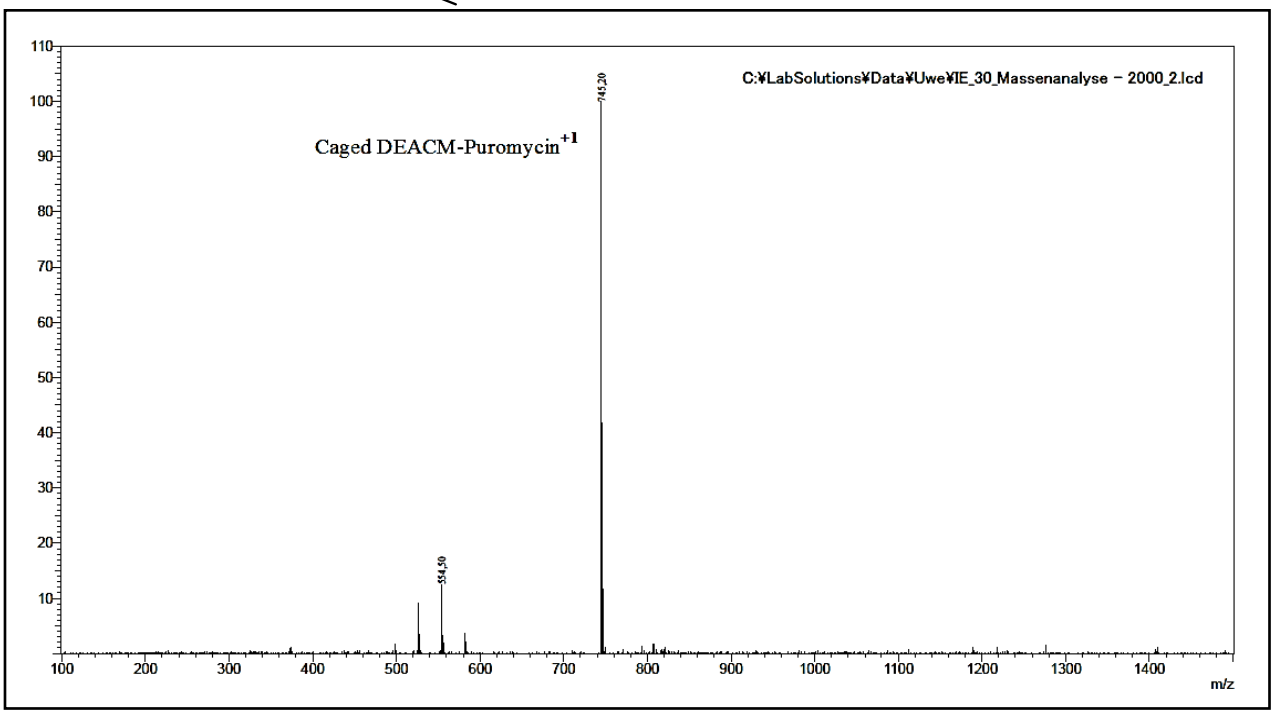

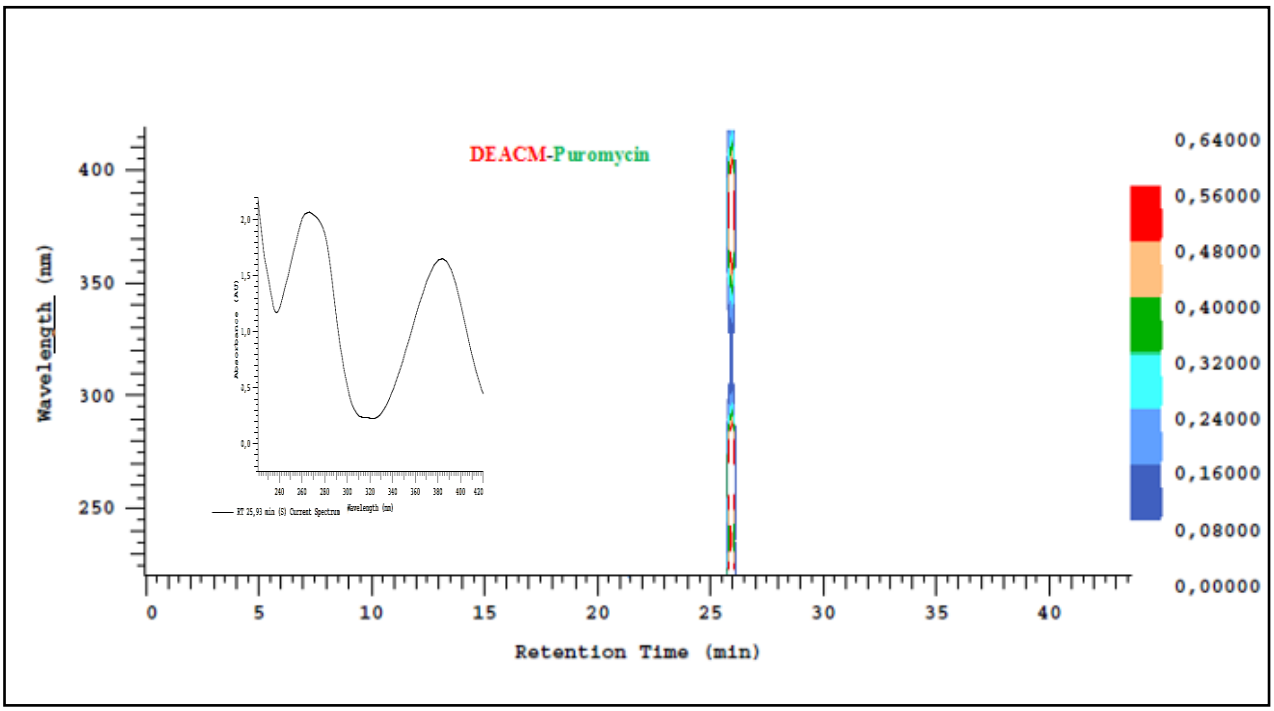

Figure S17. Mass (ESI^+) spectra, and HPLC-chromatogram of compound [**6].**

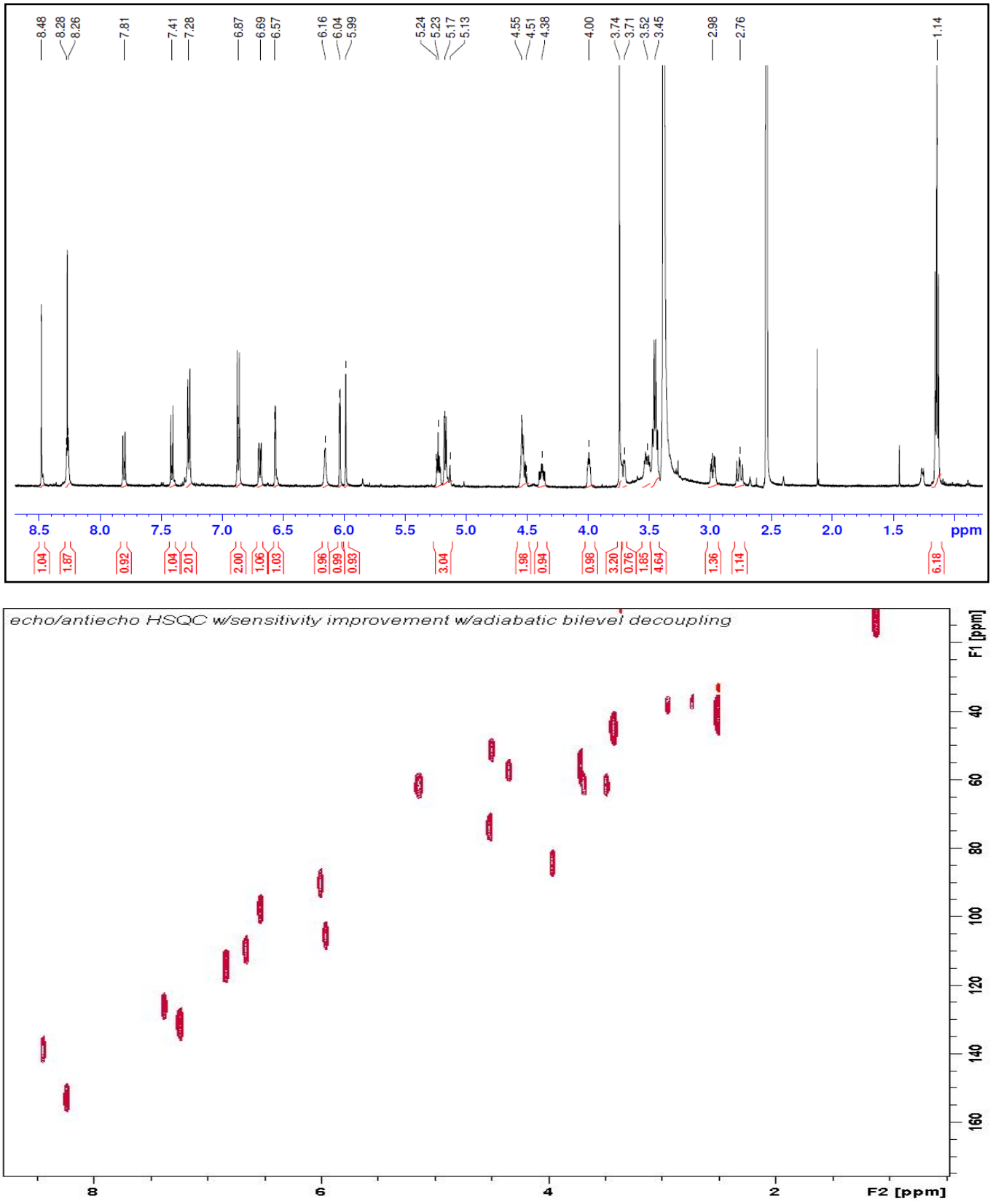

Figure S18. ^{1}H NMR and ^{1}H-^{13}C-HSQC-NMR spectra of compound [**6]**

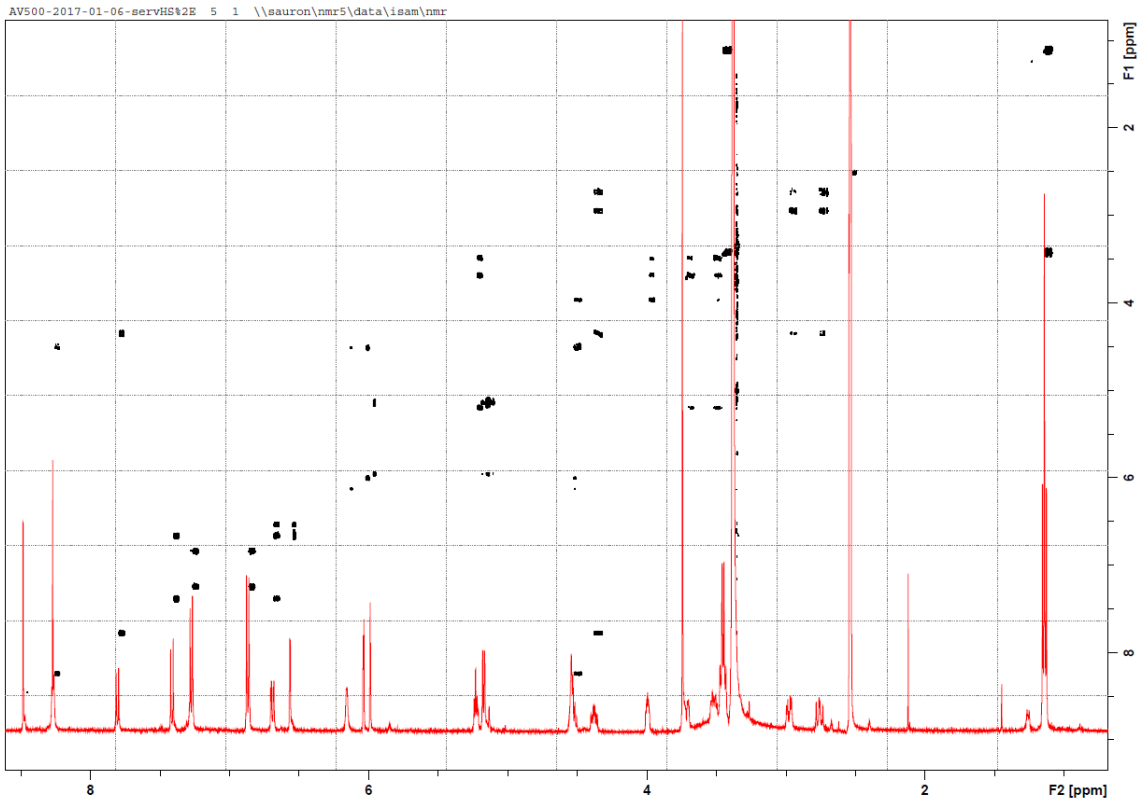

Figure S19. ^{1}H-COSY-NMR spectra of compound **[6].**